Electronic Supplementary Material (ESI) for Journal of Materials Chemistry C.
This journal is © The Royal Society of Chemistry 2024

$CaY_2ZrScAl_3O_{12}:Cr^{3+}$—An efficient and thermally stable garnet phosphor for high-performance NIR LEDs

Tianxiang Zheng,[a] Yun Ding,[a] Yihang Han,[b] Min Luo,[a] Zhihan Chu,[c] Zihao Fan,[c] Hanyu Cao,[a] Fuyun Duan,[d] and Yu Xiao*[a]

a. College of Science, Nanjing Forestry University, Nanjing 210037, P. R. China.

b. College of Chemistry and Molecular Engineering, Peking University, Beijing 100871, P. R. China.

c. College of Information Science and Technology & Artificial Intelligence, Nanjing Forestry University, Nanjing 210037, P. R. China.

d. Shandong INOV Polyurethane CO., Itd, Zibo 255000, P. R. China.

Experimental section

Material synthesis

A series of CYZS:xCr^{3+} ($0.01 \leq x \leq 0.20$ mol) samples were synthesized via a conventional high-temperature solid-state reaction. The initial raw materials including $CaCO_3$ (99.99%), Y_2O_3 (99.99%), ZrO_2 (99.99%), Sc_2O_3 (99.99%), Al_2O_3 (99.99%), and Cr_2O_3 (99.95%) were weighed by a stoichiometric ratio. These raw materials were ground in agate mortar for 30 minutes until they are thoroughly mixed, and then the mixtures were transferred into corundum crucibles and sintered at 1600 °C for 4 h in a muffle furnace. After cooling to room temperature, the samples were finely ground to obtain the fine powder for subsequent characterization. In addition, to mitigate any potential interference stemming from the impurity in CYZS:xCr^{3+}, the samples $CaAl_2O_4$:0.08Cr^{3+} and $Y_4Zr_3O_{12}$:0.08Cr^{3+} were also prepared in accordance with the relevant literatures.[1,2]

NIR pc-LED fabrication

NIR pc-LED device was fabricated using the optimal NIR phosphor CYZS:0.08Cr^{3+} and InGaN blue-LED chips (455 nm). First, the NIR phosphor CYZS:0.08Cr^{3+} was thoroughly mixed with epoxy resin. Then, the mixture was put on the InGaN blue-LED chip. Finally, the InGaN blue-LED chip (455 nm) coated the NIR phosphor should be solidified at 120 °C for 20 min.

Characterization

The Rietveld refinement of X-ray diffraction (XRD) pattern was performed by FullProf program using data collected in multifunctional horizontal X-ray diffractometer (Ultima IV, Rigaku, Japan) with Cu Kα radiation (λ = 1.54056 Å). Diffuse reflection (DR) spectra were measured using a UV-3600 plus UV–vis–NIR spectrometer (Shimadzu, Japan). The high-resolution transmission electron microscopy (HRTEM) images and elemental distributions were measured on a transmission electron microscope (JEM-2100F, UHR) and JSM-7600F (JEOL), respectively. X-ray photoelectron spectroscopy (XPS) was performed on AXIS Ultra-DLD (Shimadzu, Japan). Photoluminescence excitation spectra, photoluminescence spectra and temperature-dependent (293−473 K) spectra were recorded using an FS5 spectrometer (Edinburgh Instruments, UK). An Edinburgh Instruments FLS-1000 spectrometer was used to evaluate fluorescence decay curves. For the PL QY measurement, the sample was put inside an optical integrating sphere coupled to an Edinburgh Instruments FLS 1000 spectrometer. Electron paramagnetic resonance (EPR) spectra was recorded at room temperature on a Bruker Elexsys E580 spectrometer operating at 9.48 GHz.

The as-prepared NIR pc-LED device were recorded using a HAAS2000 photoelectric measurement system (EVERFINE, China).

Computational details

All the calculations are performed in the framework of the density functional theory with the projector augmented plane-wave method, as implemented in the Vienna ab initio simulation package.[3] The generalized gradient approximation proposed by Perdew-Burke-Ernzerhof (PBE) is selected for the exchange-correlation potential.[4] The cut-off energy for plane wave is set to 480 eV. The energy criterion is set to 10^{-5} eV in the iterative solution of the Kohn-Sham equation. All the structures are relaxed until the residual forces on the atoms have declined to less than 0.02 eV/Å.

Equation S1

$$F(R) = \frac{(1-R)^2}{2R} \tag{1}$$

$$[F(R) \times h\nu]^{1/n} = A(h\nu - E_g) \tag{2}$$

Where $F(R)$ is the absorption, R is the reflectance, $h\nu$ is the photon energy, A is the absorption constant, and E_g is the optical bandgap. The n values determined by the directly allowed transition, directly forbidden transition, indirectly allowed transition, and indirectly forbidden transition are 1/2, 3/2, 2, and 3, respectively.[5,6]

Equation S2

$$R_c = 2\left(\frac{3V}{4\pi x_c N}\right)^{1/3} \quad (1)$$

The parameters in the formula include the number of central cations in a unit cell (N), the critical concentration (x_c), and the cell volume (V). In the case of CYZS:0.08Cr^{3+}, N is equal to 8, V is equal to 1896.413 $Å^3$, and x_c is equal to 0.08. The calculation results in a value of 17.82 Å for R_c.[7]

Equation S3

$$\frac{I}{y} = \frac{k}{1+\beta(y)^{\theta/3}} \quad (2)$$

Where I is the PL intensity, y is the Cr^{3+} concentration larger than x_c = 0.08, k and β are constants, and θ is an indication of the type of electric multipolar interactions. The value of θ is 3, 6, 8, and 10, standing for the energy transfer mechanism of exchange coupling, electric dipole-dipole, dipole-quadrupole, and quadrupole-quadrupole interactions, respectively.[8,9]

Equation S4

$$10Dq = E(^4T_{2g}) \tag{1}$$

$$Dq / B = \frac{15\left(\Delta E / Dq - 8\right)}{\left(\Delta E / Dq\right)^2 - 10\left(\Delta E / Dq\right)} \tag{2}$$

$$\Delta E = E\left(^4T_{1g}\right) - E\left(^4T_{2g}\right) \tag{3}$$

Where B is the Racah parameter, $E(^4T_{1g})$ and $E(^4T_{2g})$ are the energy of $^4T_{1g}$ and $^4T_{2g}$ levels, respectively, ΔE is the energy separation between $^4T_{1g}$ and $^4T_{2g}$ energy levels.[10,11]

Equation S5

$$I(T) = \frac{I_0}{1 + A \cdot e^{(-\Delta E / k_B T)}}$$

Where I_0 is the PL intensity at 0 K, $I(T)$ is the PL intensity at a given temperature T, A is a constant, ΔE is the activation energy for thermal quenching, and k_B is the Boltzmann constant. The value of ΔE is determined to be 0.36 eV for CYZS:0.08Cr^{3+}.[12]

Table S1. Refined results of the CYZS:0.08Cr^{3+} sample

formula	CYZS
radiation type; λ (Å)	X-ray; 1.54056
2θ (degree)	10–90
temperature (°C)	25
space group	$Ia\bar{3}d$
a = b = c (Å)	12.37782
β (degree)	90.00
V (Å^3)	1896.413(0.090)
profile R-factor, R_p	0.0849
weighted profile R-factor, R_{wp}	0.1200

Table S2. PL lifetimes of Cr^{3+} in CYZS:$x$$Cr^{3+}$ (0.01 mol ≤ x ≤ 0.20 mol)

Formula	CYZS:0.01Cr^{3+}	CYZS:0.04Cr^{3+}
Fitting functions	$y = A_1 \exp(-x/t_1) + A_2 \exp(-x/t_2)$	$y = A_1 \exp(-x/t_1) + A_2 \exp(-x/t_2)$
Fitting Parameters	A_1 = 0.70; t_1 = 60.28 μs	A_1 = 0.59; t_1 = 56.30 μs
	A_2 = 0.30; t_2 = 123.25 μs	A_2 = 0.42; t_2 = 101.00 μs
Formula	CYZS:0.08Cr^{3+}	CYZS:0.12Cr^{3+}
Fitting functions	$y = A_1 \exp(-x/t_1) + A_2 \exp(-x/t_2)$	$y = A_1 \exp(-x/t_1) + A_2 \exp(-x/t_2)$
Fitting Parameters	A_1 = 0.79; t_1 = 61.26 μs	A_1 = 0.92; t_1 = 60.05 μs
	A_2 = 0.17; t_2 = 105.94 μs	A_2 = 0.07; t_2 = 120.81 μs
Formula	CYZS:0.16Cr^{3+}	CYZS:0.20Cr^{3+}
Fitting functions	$y = A_1 \exp(-x/t_1) + A_2 \exp(-x/t_2)$	$y = A_1 \exp(-x/t_1) + A_2 \exp(-x/t_2)$
Fitting Parameters	A_1 = 0.78; t_1 = 53.37 μs	A_1 = 0.89; t_1 = 54.43 μs
	A_2 = 0.20; t_2 = 86.93 μs	A_2 = 0.03; t_2 = 133.77 μs

Table S3. Crystal-field parameters in CYZS:0.08Cr^{3+}

Parameters	Value
Dq	1538.5 cm^{-1}
B	712.3 cm^{-1}
Δ*E*	6837 cm^{-1}
Dq/B	2.16

Table S4. The performances of NIR pc-LEDs using the NIR phosphors with emission peaking around ~760 (750–770 nm).

Phosphor	λ_{em} (nm)	I_{423K}(%)	IQE(%)	EQE(%)	Ref.
$CaLu_2Mg_2Si_3O_{12}:Cr^{3+}$	765	92.1@373 K	~41	20.7	13
$K_2NaScF_6:Cr^{3+}$	765	89.6	74	–	14
$Sr_3Sc_4O_9:Cr^{3+}$	761	70.4@373 K	87	–	15
$Y_3In_2Ga_3O_{12}:Cr^{3+}$	760	100	91.6	42.7	5
$Gd_3Sc_{0.5}Al_{1.5}Ga_3O_{12}:Cr^{3+}$	754	90.7	47.2	754	16
$Y_3Sc_2Al_3O_{12}:Cr^{3+}$	753	97	74	31	17
$CaLu_2Mg_2Si_3O_{12}:Cr^{3+}$	750	50@578 K	85.7	38.6	10
$Y_2Mg_2Al_2Si_2O_{12}:Cr^{3+}$	750	89@373 K	79	–	18

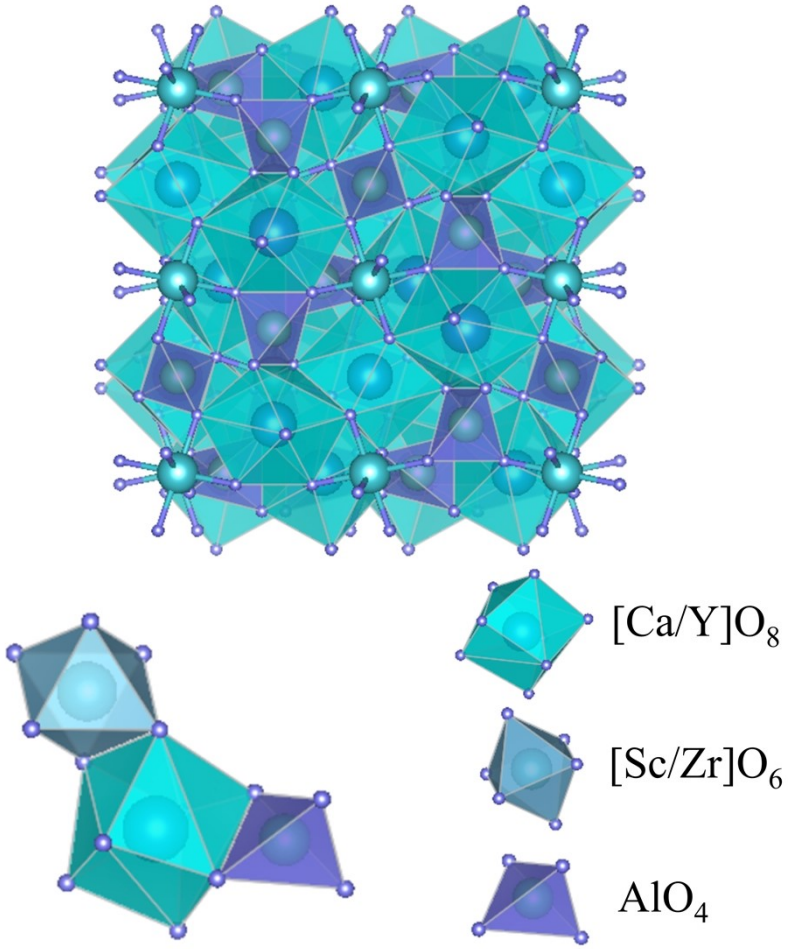

Figure S1. The crystal structure of CYZS.

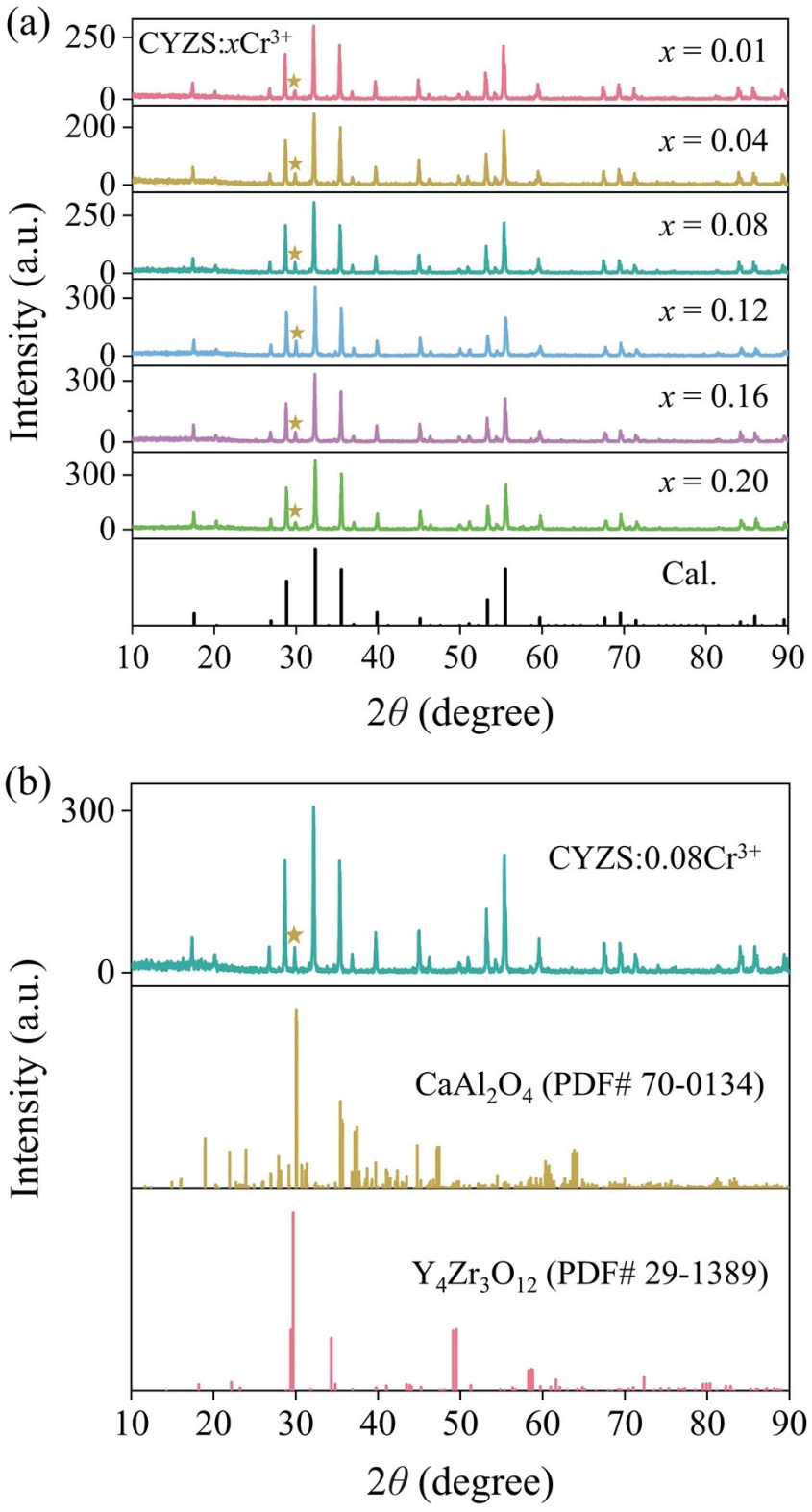

Figure S2. (a) XRD patterns of CYZS:xCr^{3+} (0.01 mol ≤ x ≤ 0.20 mol); (b) XRD pattern of CYZS:0.08Cr^{3+} phosphor.

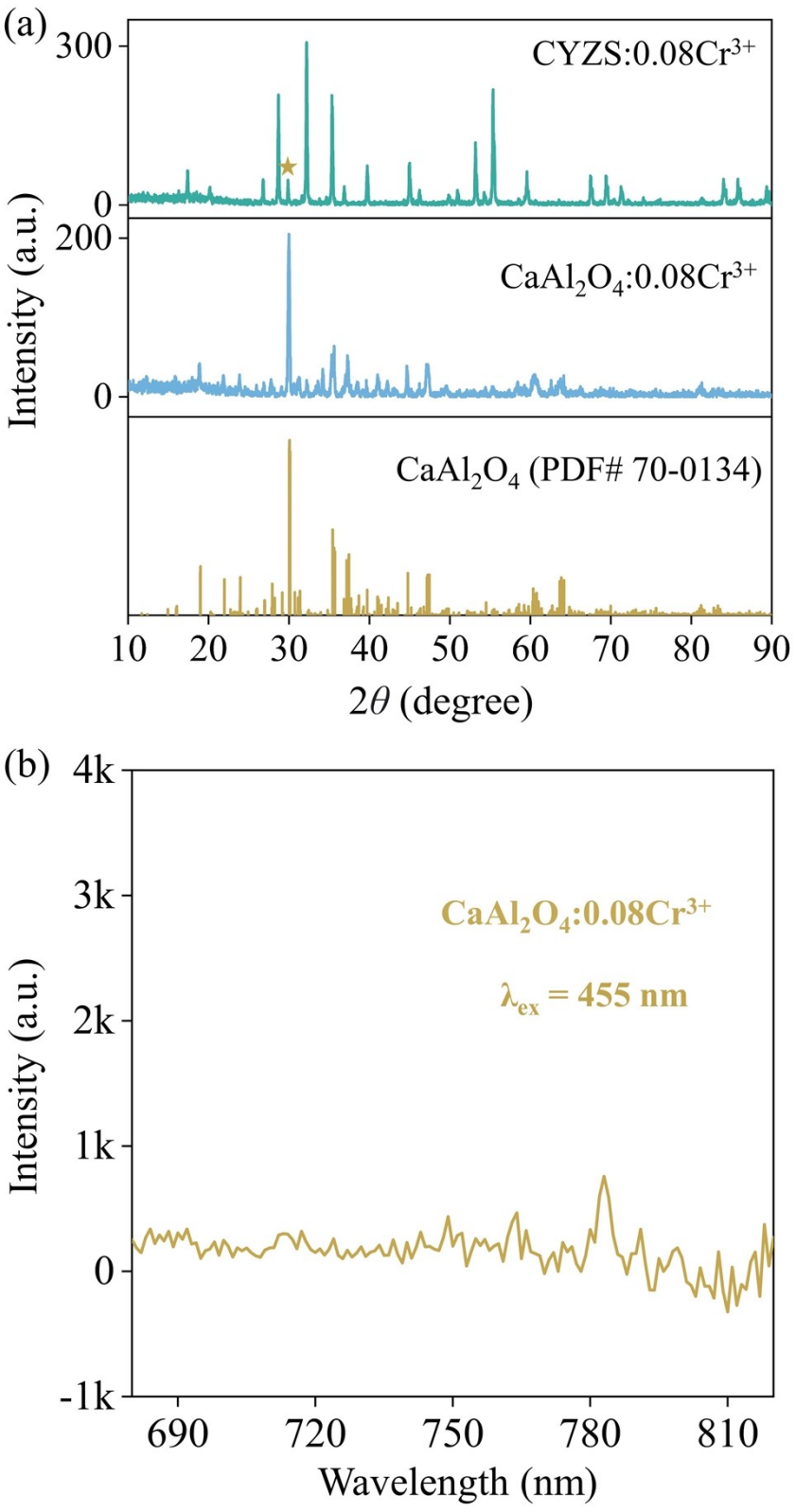

Figure S3. (a) XRD patterns; and (b) emission spectra of $CaAl_2O_4$:0.08Cr^{3+}.

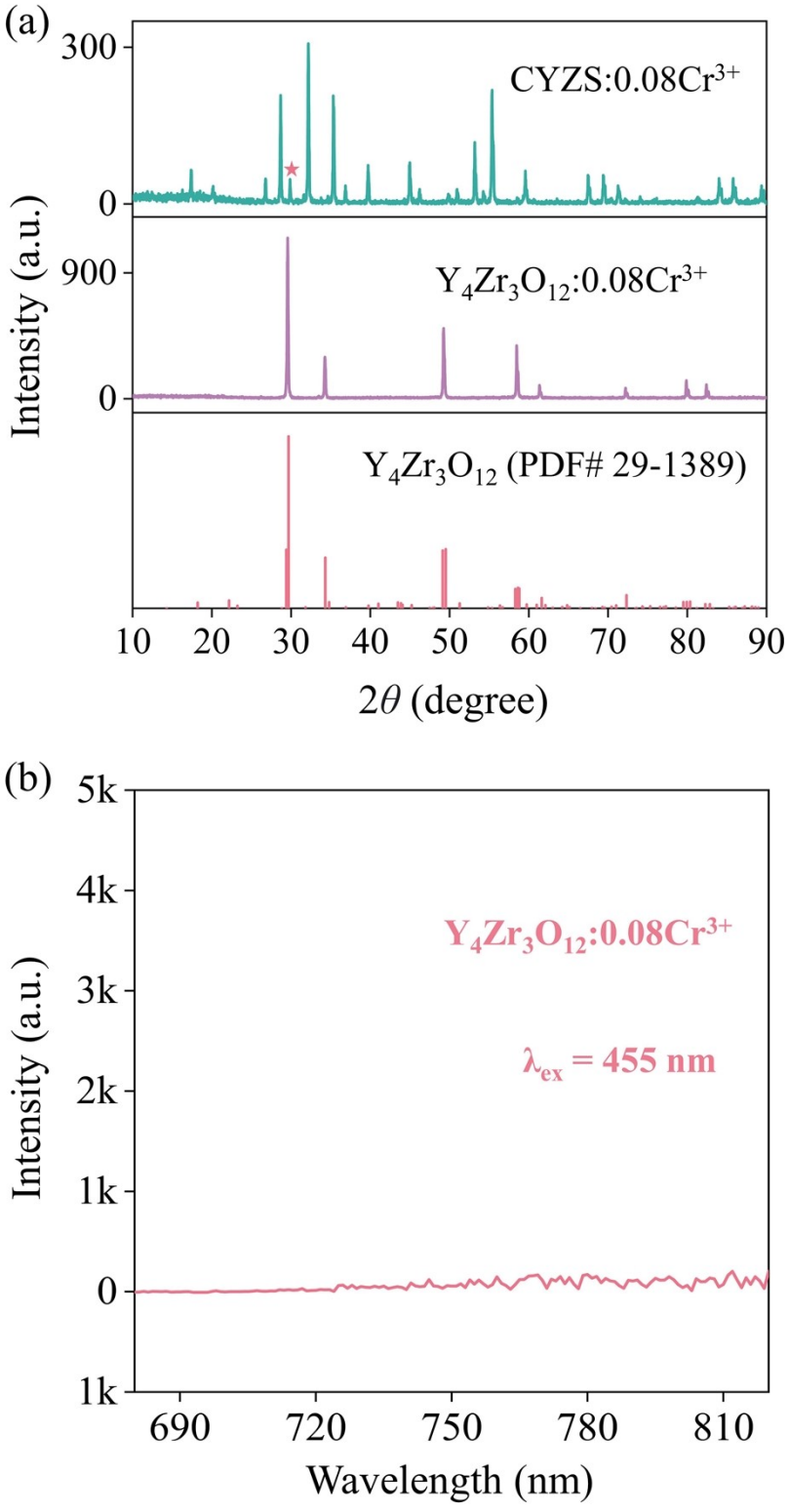

Figure S4. (a) XRD patterns; and (b) emission spectra of $Y_4Zr_3O_{12}$:0.08Cr^{3+}.

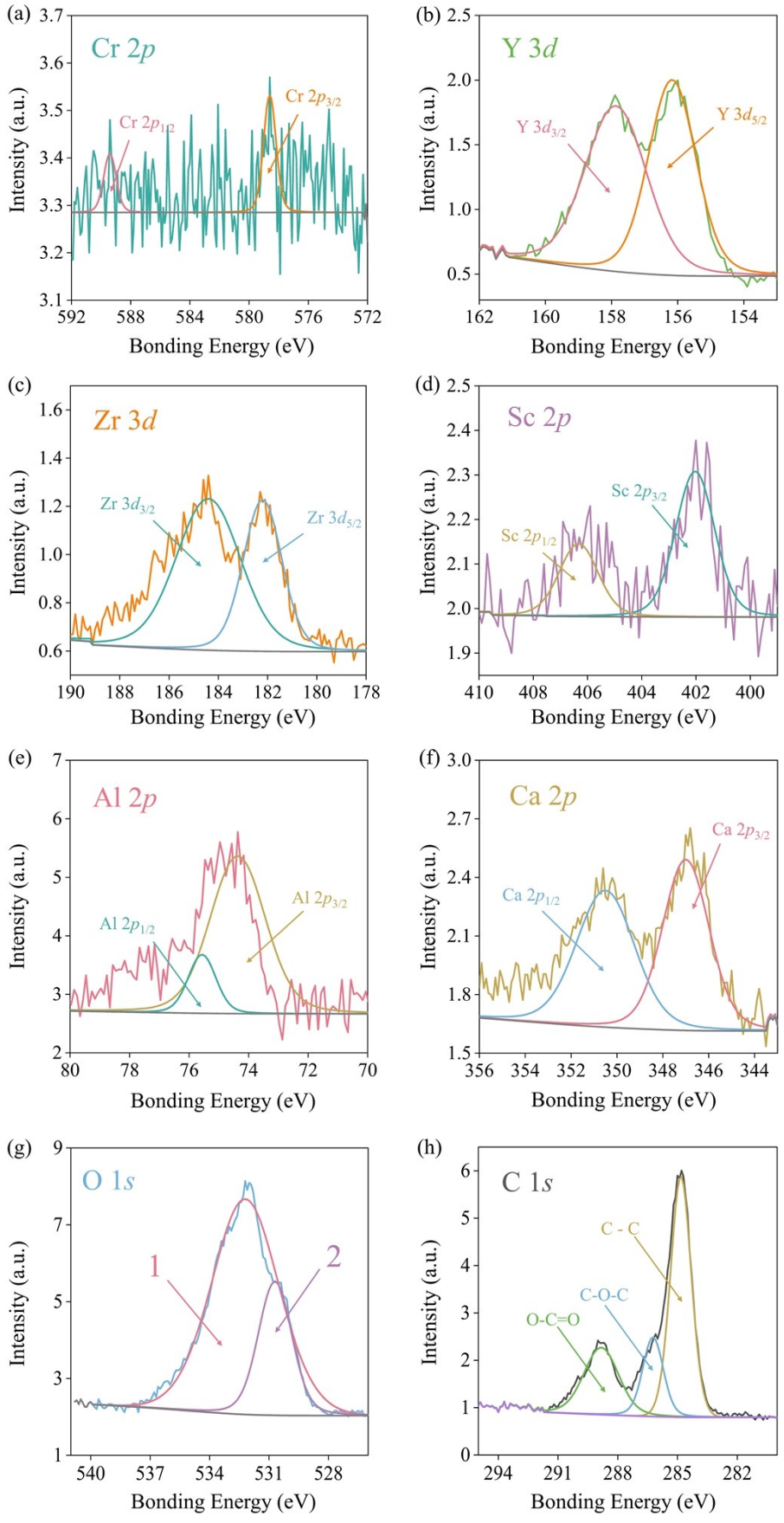

Figure S5. XPS spectra of Cr, Ca, Y, Zr, Sc, Al, O and C elements in CYZS:0.08Cr^{3+}.

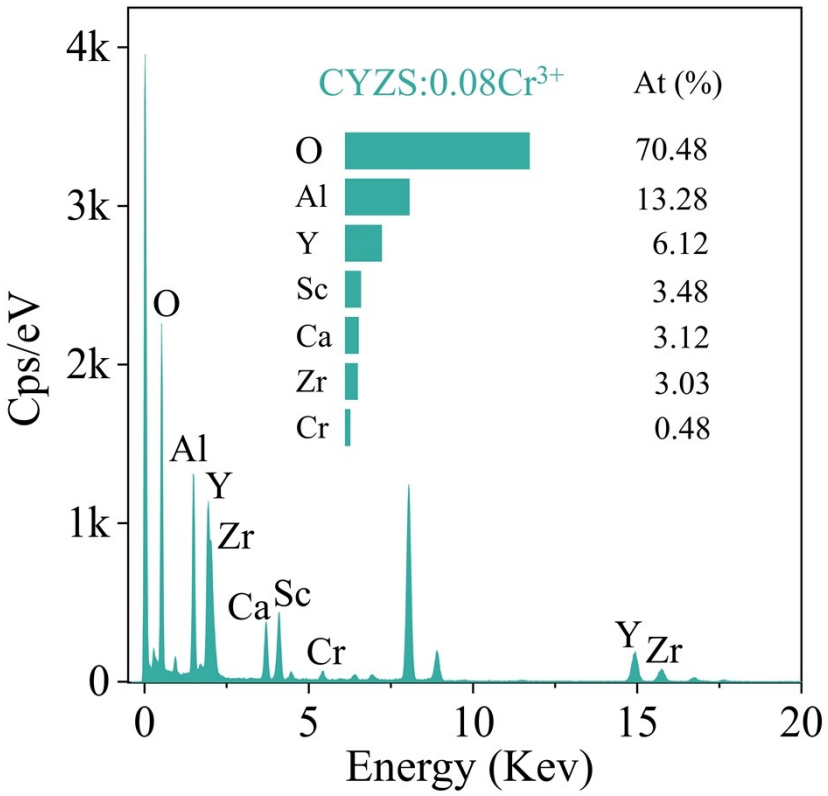

Figure S6. EDS image of CYZS:0.08Cr^{3+}.

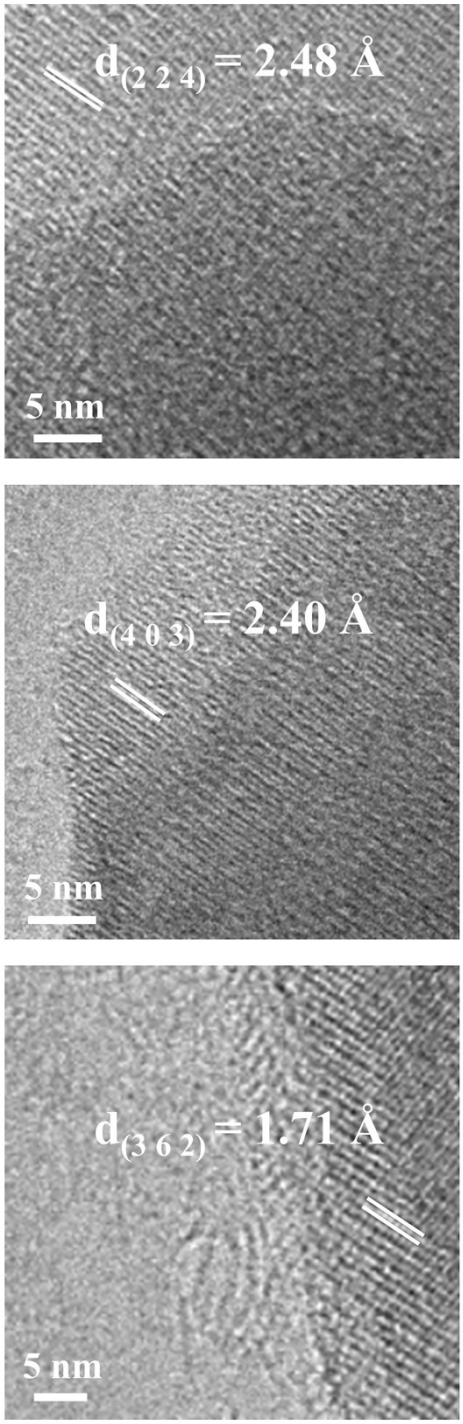

Figure S7. HRTEM images of CYZS:0.08Cr^{3+}.

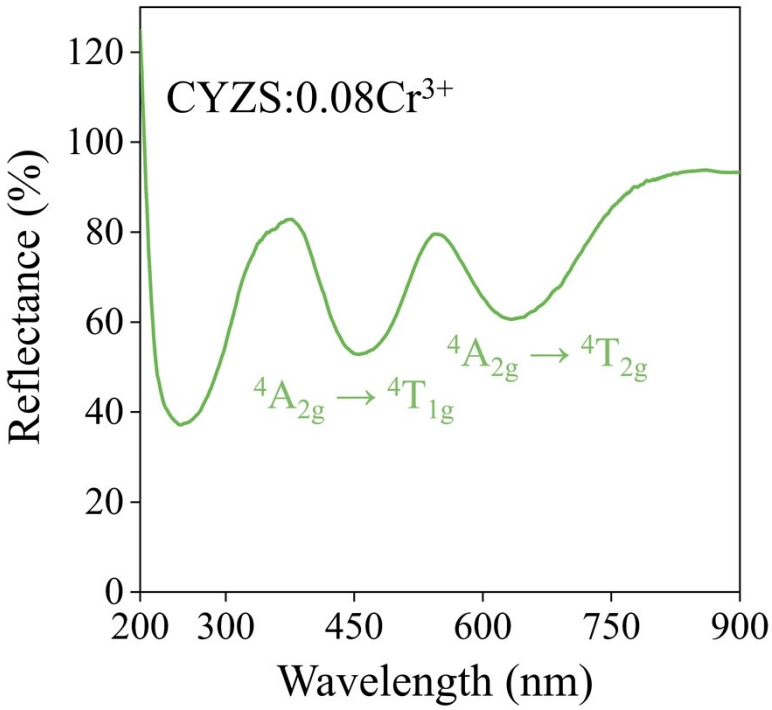

Figure S8. DR spectra of CYZS:0.08Cr^{3+}.

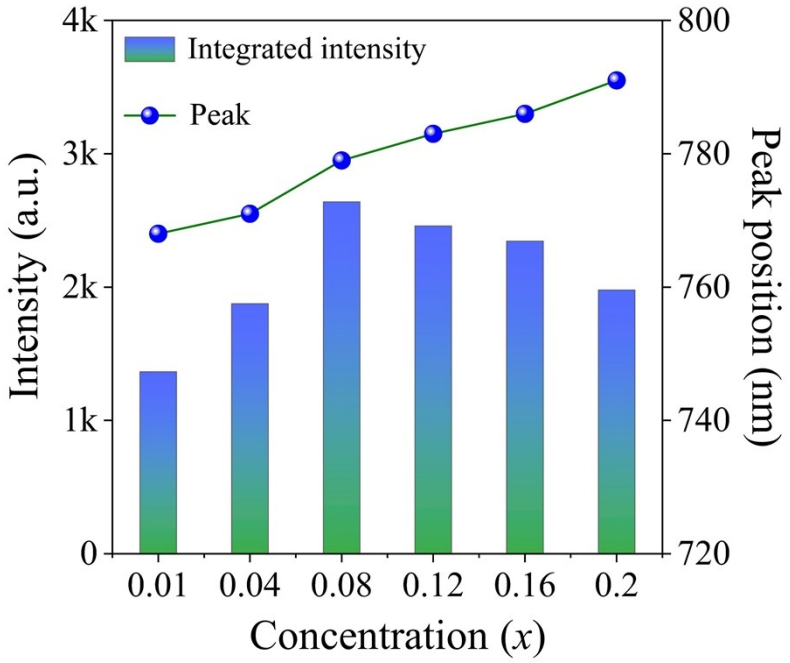

Figure S9. Integrated emission intensity and peak position of CYZS:xCr^{3+} (0.01 mol ≤ x ≤ 0.20 mol).

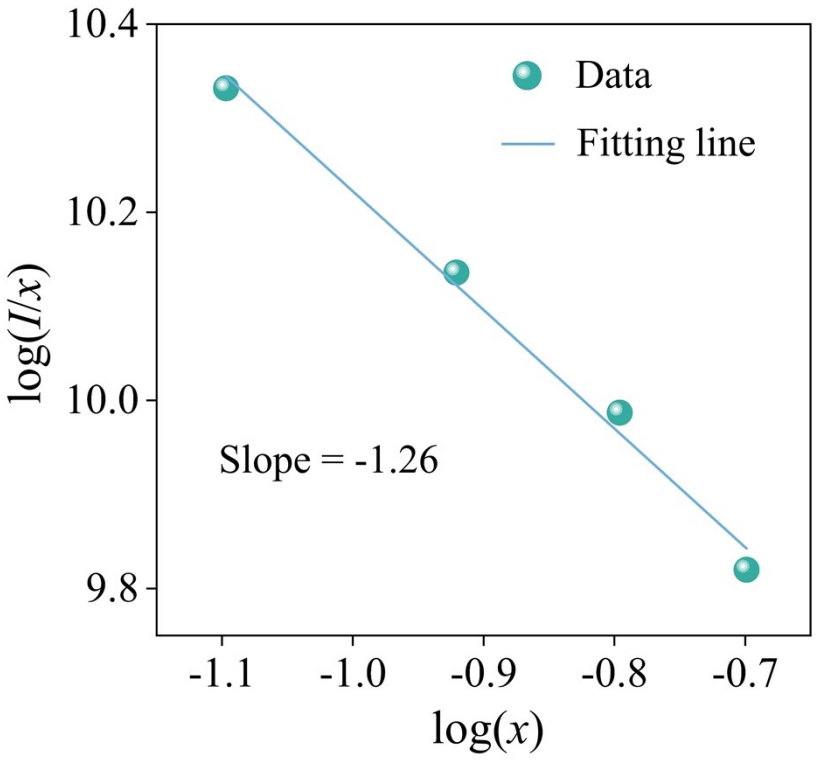

Figure S10. Linear fitting of log(*I*/*x*) versus log(*x*) for CYZS:*x*Cr^{3+} (0.08 mol ≤ *x* ≤ 0.20 mol); Based on Equation S3, the energy transfer mechanism involves interactions between adjacent Cr^{3+} ions in CYZS, evidenced by the θ value of 3.8, which closely aligns with the value of θ = 3, consistent with previous reports.[19,20]

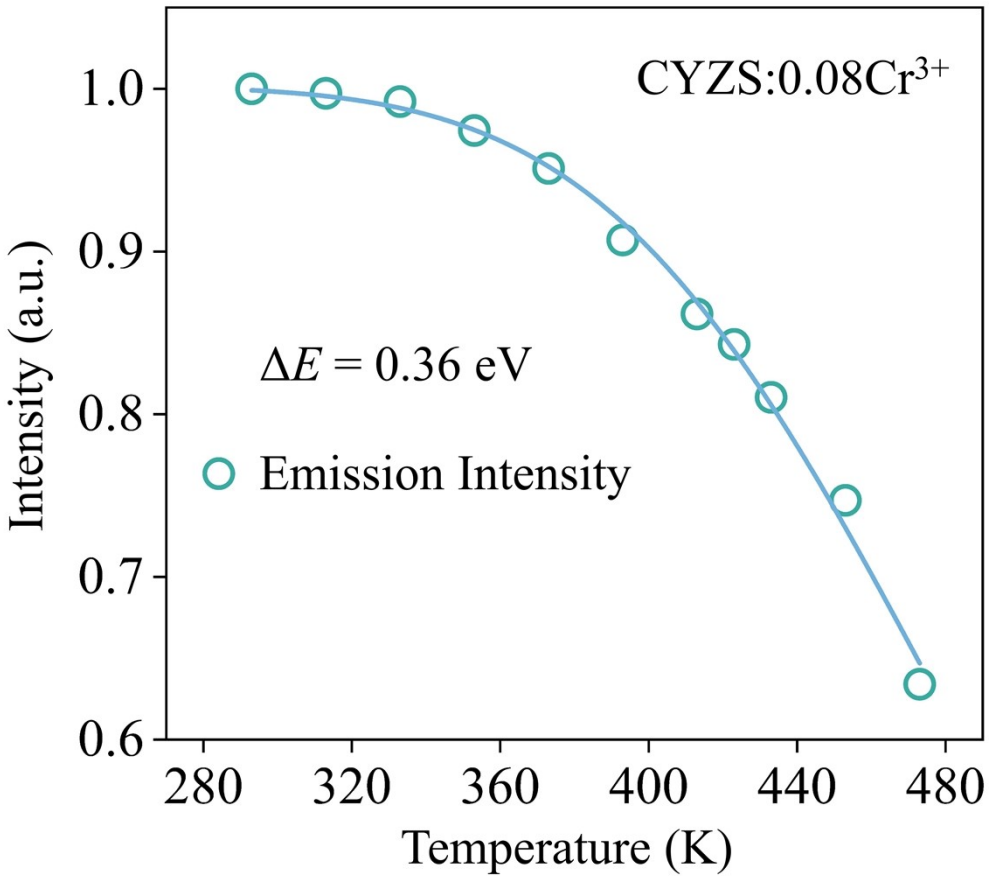

Figure S11. Normalized total emission intensity versus the heating temperature.

References

1. H. Ryu and K. S. Bartwal, *J Alloy. Compd.*, 2008, **464**, 317–321.
2. J. Y. Park and H. K. Yang, *Dyes Pigments*, 2017, **141**, 348–355.
3. G. Kresse and D. Joubert, *Phys. Rev. B* 1999, **59**, 1758–177.
4. J. P. Perdew, K. Burke and M. Ernzerhof, *Phys. Rev. Lett.*1996, **77**, 3865–3868.
5. C. Li and J. Zhong, *Chem. Mater.*, 2022, **34**, 8418–8426.
6. S. Devi, A. Khatkar, V. B. Taxak, M. Dalal, S. Chahar, J. Dalal and S. P. Khatkar, *J Alloy. Compd.*, 2018, **767**, 409–418.
7. Blasse G. Phys Lett, 1968, **28**, 444–5.
8. L. G. Van Uitert, *J Electrochem Soc*, 1967, **114**, 1048.
9. L. G. Van Uitert and L. F. Johnson, *The Journal of Chemical Physics*, 1966, **44**, 3514–3522.
10. H. Xiao, J. Zhang, L. Zhang, H. Wu, H. Wu, G. Pan, F. Liu and J. Zhang, *Adv. Opt. Mater.*, 2021, **9**, 202101134.
11. H. Zhang, J. Zhong, F. Du, L. Chen, X. Zhang, Z. Mu and W. Zhao, *ACS Appl. Mater. Interfaces*, 2022, **14**, 11663–11671.
12. K. J. Laidler, *J. Chem. Educ.*, 1984, **61**, 494.
13. R. Li, Y. Liu, C. Yuan, G. Leniec, L. Miao, P. Sun, Z. Liu, Z. Luo, R. Dong and J. Jiang, *Adv. Opt. Mater.*, 2021, **9**, 202100388.
14. E. Song, H. Ming, Y. Zhou, F. He, J. Wu, Z. Xia and Q. Zhang, *Laser Photonics Rev*, 2020, **15**, 202000410.
15. J. Lin, L. Zhou, L. Ren, Y. Shen, Y. Chen, J. Fu, L. Lei, R. Ye, D. Deng and S. Xu, *J Alloy. Compd.*, 2022, **908**, 164582.
16. X. Wu, Z. Luo, Y. Zhuang, Z. Liu, P. Sun, Y. Liu, L. Zhang, H. Qin and J. Jiang, *Ceram Int*, 2023, **49**, 21688–21694.
17. H. Li, J. Jiao, X. Xiang, J. Wu, W. Hu, J. Xie, S. Huang, H. Zhang and J. Zhu, *Adv. Opt. Mater.*, 2024, **12**, 202302391.
18. Y. Sun, M. Shang, Y. Wang, Y. Zhu, X. Xing, P. Dang and J. Lin, *J. Mater. Chem. C*, 2024, **12**, 2814–2823.
19. Y. Jin, Z. Zhou, R. Ran, S. Tan, Y. Liu, J. Zheng, G. Xiang, L. Ma and X. j. Wang, *Adv. Opt. Mater.*, 2022, **10**, 202202049.

20. Y. Zhang, Z. Gao, Y. Li, S. Chen, M. Han, J. Li, Q. Zhang, Y. Shen, D. Deng and S. Xu, *Inorg. Chem.*, 2023, **62**, 17371–17381.